Experimental report

13/02/2019

Proposal: 9-11-1851 **Council:** 4/2017

Title: Probing the Spatial Ordering and Orientation of Block Copolymer Nanodomains On a Layer of Cross-Linked Homopolymer by Grazing Incident Small

Research area: Materials

This proposal is a new proposal

Main proposer: Chun-Ming WU

Experimental team: Yi-Fang CHEN
Ya-Sen SUN
Iris CHANG
Chun-Ming WU

Local contacts: Lionel PORCAR

Samples: Poly(methyl methacrylate) / (C5O2H8)n
Polystyrene / C8H8)n
d-Polystyrene / (C8D8)n

Instrument	Requested days	Allocated days	From	To
D22	6	3	12/10/2018	15/10/2018

Abstract:

In this proposal, we aim to understand how the diffusion and penetration depth of block copolymer (BCP) chains within a PS layer with varied cross-linking densities influence the spatial ordering and orientation of BCP nanodomains at an elevated temperature using grazing incident small angle neutron scattering (GISANS) technique. The motion of polymeric chains will be controlled by thermal annealing at 210 and 230 oC. To gain an in-depth understanding of correlations between penetration length and cross-linking density, we will characterize PS-b-PMMA thin films of different MWs on a layer of dPS with different cross-linking densities after thermal annealing of varying durations at 210 and 230 oC.

Report for No. 9-11-1851

Probing the Spatial Ordering and Orientation of Block Copolymer Nanodomains On a Layer of Cross-Linked Homopolymer by Grazing Incident Small

Background

A skin layer (1.6 nm at most) of a neutral surface of PS was obtained with an optimum oxidation via brief UVI in air (UVIA). UVI in an inert environment (gaseous dinitrogen) (UVIN) stabilized the PS layers via cross-linking and enabled the PS networks to have an effective adhesive contact with the underlying substrate.[1] Thorough examination of domain orientations and spatial orders of 230 °C-thermally-annealed polystyrene-*block*-poly(methyl methacrylate), (PS-*b*-PMMA), thin films in a series on the UVI-treated PS layers yielded clear evidence that a dense layer of neutralized PS chains was required for the perpendicular orientation of PS-*b*-PMMA nanodomains. In particular, in addition to neutralization, two factors – the densities of physical entanglements and of chemical crosslinks – both in UVI-treated PS, should be considered for the perpendicular orientation of nanolamellae in symmetric PS-*b*-PMMA thin films. The density of physical entanglement (Σ_p) in PS depended intrinsically on M_n of the PS whereas the density of chemical crosslinks (Σ_c) was controlled with a varied duration of UVIN. Sufficiently large densities of physical entanglements and chemical crosslinks can prevent PS-b-PMMA chains from penetrating through the neutral skin layer. The total density (Σ) of physical entanglements and chemical crosslinks required for the perpendicular orientation correlated with the dimensions of the PS-*b*-PMMA chains. Understanding the structural evolution and dynamics of PS-b-PMMA chains at a neutralized surface of UVI-treated PS is crucial to the optimization of controlling polymer-surface interactions with UVI-treated PS layers but nevertheless still an open question.

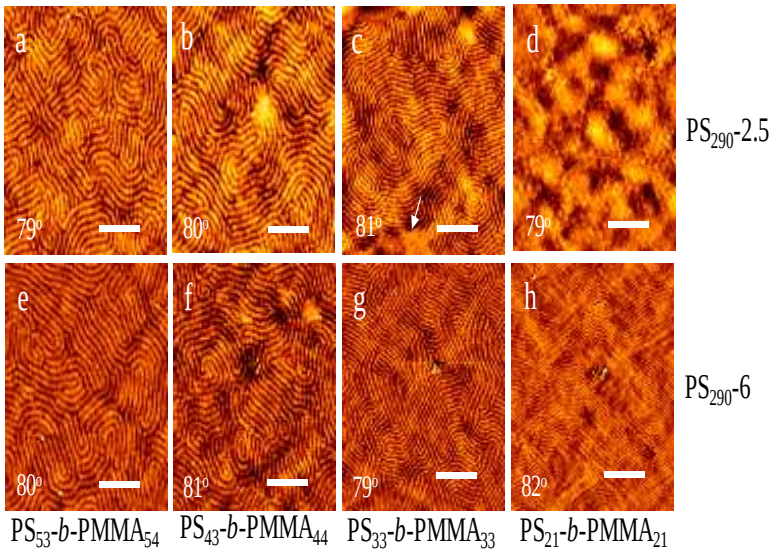

Figure 1. AFM topographic images (2×2 μm^2) of lamellar nanodomains of symmetric BCP, (a, e) PS_{53}-*b*-$PMMA_{54}$, (b, f) PS_{43}-*b*-$PMMA_{44}$, (c, g) PS_{33}-*b*-$PMMA_{33}$ and (d, h) PS_{21}-*b*-$PMMA_{21}$, on top of (a-d) PS_{290}-2.5 and (e-f) PS_{290}-6 layers with UVIN (2.5 and 6h). The arrowhead shown in image c indicates a defect. The values specify the contact angle of water on the UVI-treated PS layers. Scale bar: 500 nm. Before AFM measurements, the PS-*b*-PMMA films were isothermally annealed at 230 °C (24 h).

Figure 1 show the surface morphology of the PS-*b*-PMMA lamellae of various sizes on PS_{290} with a neutral surface treated with UVIN for 2.5 and 6 h. Σ were approximately 1.55×10^4 mol cm^{-3} and 1.98×10^4 mol cm^{-3} respectively for PS_{290}-2.5 and PS_{290}-6 with a neutral surface. As shown in Figure 1, regardless of the duration of UVIN, both PS_{53}-b-$PMMA_{54}$ and PS_{43}-b-$PMMA_{44}$ display a morphology of perpendicular orientation. In comparison, PS_{33}-b-$PMMA_{33}$ shows a mixed orientation of standing and lying with defects on PS_{290}-2.5 but a perpendicular orientation on PS_{290}-6. A featureless morphology was obtained for PS_{21}-b-$PMMA_{21}$ on PS_{290}-2.5 whereas a perpendicular orientation was obtained for PS_{21}-b-$PMMA_{21}$ on PS_{290}-6. The result indicates that the increased Σ in PS can improve the perpendicular orientation of nanolamellae.

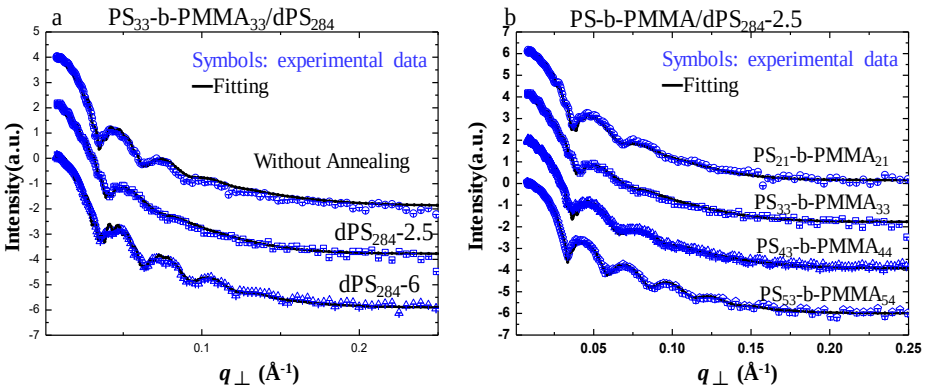

Figure 2. (a) Static NR data (symbols) and fitted curves (lines) of PS_{33}-b-$PMMA_{33}$ films with thermal annealing at 230 °C on dPS_{284}-2.5 and dPS_{284}-6. For comparison, the NR datum and fitted curve of the pristine PS_{33}-b-$PMMA_{33}$ on dPS_{284}-2.5 were plotted together. (b) Static NR data (symbols) and fitted curves (lines) of PS-b-PMMA films of different MWs with thermal annealing at 230 °C on dPS_{284}-2.5.

Figure 2a shows the static NR data as well as fit curves for the PS_{33}-b-$PMMA_{33}$ films on the neutralized dPS_{284}-2.5 and dPS_{284}-6 after thermal annealing at 230 °C (24h). For comparison, the static NR curve and the best fit curve of the as-spun PS_{33}-b-$PMMA_{33}$ film on the neutralized PS_{284}-2.5 were shown together in Figure 2a (top curve). In the as-spun PS_{33}-b-$PMMA_{33}$ film on PS_{284}-2.5 without 230 °C-thermal annealing, several distinct interference fringes with two different frequencies in the reflectivity curve are observed indicating that the interface is sharp defined. The low-frequency fringes with enhanced intensity correspond to the thickness of the dPS layer while the high-frequency fringes with small intensity are associated with the thickness of the PS_{33}-b-$PMMA_{33}$ films. The reason is that dPS has a much higher SLD value than PS-b-PMMA. The initial thickness of the dPS layer as well as PS-b-PMMA film determines the frequency between the maxima of the reflectivity curve. As the specimens were annealed, the interface between the bilayers (PS-b-PMMA/dPS) begins to broaden and results in a gradual loss of the higher order maxima in the NR curves at high q values (Figure 2). The loss of higher order maxima is more obvious for the PS_{33}-b-$PMMA_{33}$ film on PS_{290}-2.5 than for that on PS_{290}-6 (Figure 2a). Such oscillation damping is also obvious for the PS_{21}-b-$PMMA_{21}$ with thermal annealing at 230 °C on dPS_{284}-2.5 (see Figure 2b). This feature implies that the PS_{21}-b-$PMMA_{21}$ chains penetrated through the PS_{284}-2.5 layer at a high diffusion rate. Annealing at 230 °C imparts the ability of motion for PS-b-PMMA chains with polymer chains of small dimensions. If the small chains can completely penetrate through the neutral layer of skin, they can experience the underlying pristine property in PS so that a mixed orientation or parallel orientation is dominant over a perpendicular orientation. Such a mixed orientation or parallel orientation depends on the depth to which the small BCP chains penetrate through the skin neutral layer. From the perspective, Figure 3 reports a collection of AFM images showing the orientation of the PS_{33}-b-$PMMA_{33}$ and PS_{21}-b-$PMMA_{21}$ nanolamellae with thermal annealing at 230 °C of duration 1, 6 and 12 h on neutralized PS_{290}-2.5.

As Figure 3 shows, with a small duration of annealing at 230 °C, the PS_{33}-*b*-$PMMA_{33}$ chains were still trapped in the neutral skin layer so as to form perpendicularly oriented nanolamellae without the presence of a lying orientation. In contrast, upon prolonged annealing of 230 °C on PS_{21}-b-$PMMA_{21}$ domain orientation would change from perpendicular to parallel, evidenced by a featureless morphology (see Figures 1d&3f). Since specular neutron

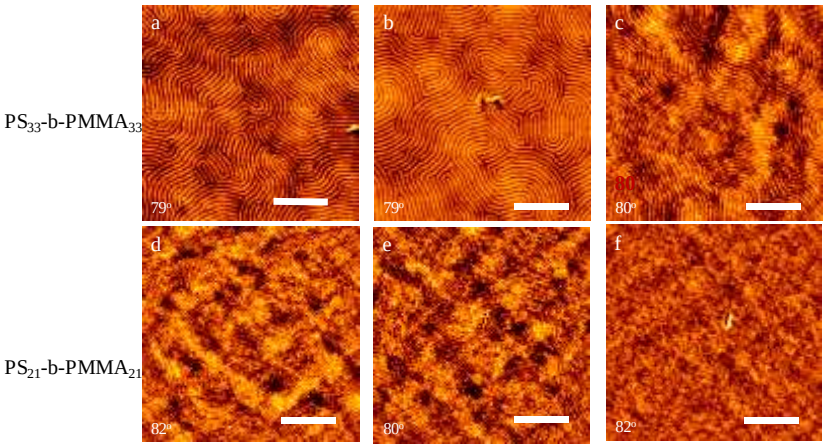

Figure 3. AFM topographic images (2×2 μm^2) of lamellar nanodomains of (a-c) PS_{33}-*b*-$PMMA_{33}$ and (d-f) PS_{21}-*b*-$PMMA_{21}$ films with annealing at 230 °C of varied duration: (a, d) 1, (b, e) 6 and (c, f) 12h on top of PS_{290}-2.5. The values denote the contact angle of water on the UVI-treated PS layers. Scale bar: 500 nm.

reflectivity is only allowable for the detection of the density profile and "blind" to lateral structures, GISANS provides an accesss to probe lateral structures. Further, although the spatial orientation and ordering of self-assembled nanodomains within thin films could be identified by grazing incidence small-angle X-ray scattering (GISAXS). Nevertheless, the local structural information, particularly at the interface between the BCP film and the cross-linked PS (or dPS), has not been well resolved yet. The reason is that those polymeric materials have similar scattering length density values under X-rays and that thus post-sample treatments are necessary to additionally remove the PMMA block for improving the scattering contrast and signals. Such as polymer degradation with UV exposure, the local structural information would be missed. This situation will call a high demand for using GISANS.

In this experiment, D22 was employed for understanding the penetration behaviour between the BCP thin film and the UV-treated PS layer. As shown in Figure 4 we successfully obtained GISANS patterns for structural evolution of dPS_{47}-*b*-$PMMA_{50}$ with thermal annealing of varied time periods on PS_{290}-2.5. As shown in Figure 4, the resulting scattering patterns are anisotropic and typically exhibit a Yoneda streak and a specular rod at q_y=0. Without thermal annealing, dPS-b-PMMA shows weak difftraction signals symmtrically locating the both sides of the specular rod (Figure 4a). Upon thermal annealing, the diffraction signals appear strong intensity and their positions display the q_y ratio of 1:2 (Figure 4b-e). The diffraction signals correspond to the formation of lamellae with a perpendicular

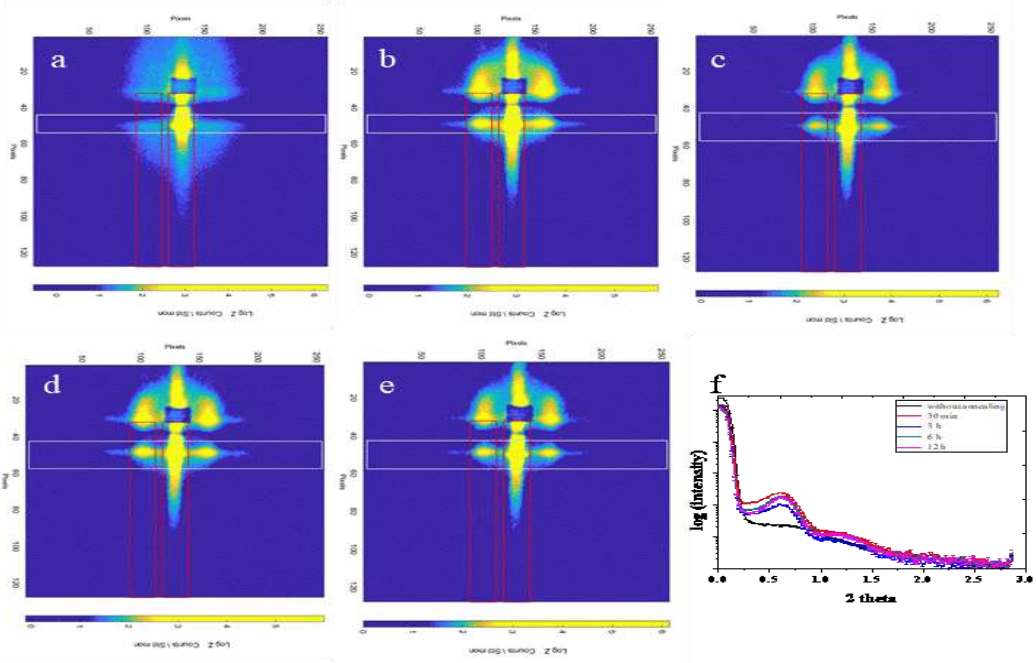

Figure 4. 2D GISANS 2D patterns (a-e) for dPS_{47}-b-$PMMA_{50}$ (a) with and with thermal annealing of varied durations: (b) 30 min, (c) 3h, (d) 6h and (e) 12h on PS_{290}-2.5. (f) correspoding 1D GISANS profiles with in-plane scan cuts along the Yoneda streak. (D_{22}; ILL, Grenoble, France, 2018).

orientation.

We plan to continue GISANS characterization on dPS-*b*-PMMA thin films of different MWs on a layer of PS with different cross-linking densities after thermal annealing of varying durations at an elevated temperature. To have a comprehensive understand how the spatial orientation and ordering of self-assembled BCP nanodomains influence by the diffusion and penetration of BCP chains within a PS layer with varied cross-linking densities at an elevated temperature. The GISANS data will be further analyzed using the GISAXS software package for the out-of-plane and lateral ordering analysis.

Reference:

[1]Y. S. Sun, C. T. Wang, J .Y. Liou, Soft Matter, 2016, 12, 2923-2931.